

# Finding graph isomorphisms in heated spaces in almost no time\*

Sara Najem

Department of Physics, CAMS  
 American University of Beirut, Lebanon  
 sn62@aub.edu.lb

Amer E. Mouawad

Department of Computer Science  
 American University of Beirut, Lebanon  
 aa368@aub.edu.lb

## Abstract

Determining whether two graphs are structurally identical is a fundamental problem with applications spanning mathematics, computer science, chemistry, and network science. Despite decades of study, graph isomorphism remains a challenging algorithmic task, particularly for highly symmetric structures. Here we introduce a new algorithmic approach grounded in spectral graph theory and discrete geometry that constructs vertex correspondences using curvature-derived, multi-scale signatures. Each vertex is assigned a canonical curvature signature built from heat-kernel coefficients organized over its breadth-first search tree, yielding a rich local invariant that can be matched globally across graphs.

Any correspondence produced by the algorithm is explicitly verified, ensuring one-sided correctness: non-isomorphic graphs are never incorrectly identified as isomorphic. Although the method does not yet guarantee success on all isomorphic inputs, we find that it correctly resolves every instance tested within deterministic polynomial time, including a broad collection of graphs known to be difficult for classical spectral and refinement-based techniques. These results demonstrate that enriched, geometry-informed spectral invariants can be substantially more discriminative than eigenvalues alone, and suggest a promising direction for practical progress on the graph isomorphism problem.

**Keywords:** graph isomorphism; spectral geometry; Laplacian heat kernel; discrete curvature; symmetry breaking

---

\*Source code for our implementation will be made available at <https://github.com/s-najem/Isomorphism-Graph-Curvature>.

# Contents

<b>1</b>	<b>Introduction</b>	<b>3</b>
<b>2</b>	<b>Background</b>	<b>4</b>
2.1	Spectral graph theory, Laplacians, and heat kernels . . . . .	4
2.2	Spectral invariants and graph isomorphism . . . . .	4
2.3	Structural restrictions and the complexity of graph isomorphism . . . . .	5
2.4	From spectra to geometry . . . . .	5
<b>3</b>	<b>The base algorithm</b>	<b>6</b>
<b>4</b>	<b>Handling degeneracies</b>	<b>8</b>
4.1	Stretching geometry using edge subdivisions . . . . .	8
4.2	Handling large groups of equal curvature via vertex identification . . . . .	9
<b>5</b>	<b>The proposed complete algorithm for graph isomorphism</b>	<b>10</b>
<b>6</b>	<b>Computational complexity</b>	<b>11</b>
6.1	Complexity of the base algorithm . . . . .	11
6.2	Complexity of handling degeneracies . . . . .	12
6.3	Complexity of the full BFS-curvature-signature algorithm . . . . .	13
<b>7</b>	<b>Experimental results</b>	<b>14</b>
7.1	Random geometric graphs . . . . .	17
7.2	Power-law cluster graphs . . . . .	18
7.3	Stochastic block graphs . . . . .	19
7.4	Regular graphs . . . . .	20
7.5	Albert-Barabasi graphs . . . . .	20
7.6	Watts-Strogatz graphs . . . . .	22
7.7	Erdos-Renyi graphs . . . . .	23
7.8	Tree graphs . . . . .	24
7.9	Paley graphs . . . . .	25
<b>8</b>	<b>Conclusion and future work</b>	<b>27</b>

# 1 Introduction

Determining whether two graphs are structurally identical is a central problem in theoretical computer science, with applications spanning chemistry, physics, network science, and data analysis. The *graph isomorphism* (GI) problem asks whether there exists a bijection between the vertex sets of two graphs that preserves adjacency. Despite decades of study, the precise computational complexity of GI remains unresolved. While the problem is known to lie in NP, it is neither known to be NP-complete nor solvable in polynomial time in full generality.

A major milestone was achieved by Babai, who showed that GI can be solved in quasipolynomial time for general graphs [4]. Nevertheless, all currently known polynomial-time algorithms apply only to restricted graph families characterized by strong structural constraints, such as bounded degree [13], bounded genus [12], bounded eigenvalue multiplicity [5], or bounded treewidth [11]. These results suggest that existing approaches rely heavily on combinatorial regularity or locality, leaving open the question of whether fundamentally different sources of structure can yield efficient isomorphism tests.

In this work, we introduce a new algorithmic approach to graph isomorphism grounded in *spectral geometry*. Rather than exploiting combinatorial restrictions, our method draws on ideas from non-commutative geometry and spectral graph theory, using curvature derived from Laplacian spectra as a tool for symmetry breaking. The conceptual foundation of our approach is inspired by recent work on geometric features of networks based on Connes’ spectral triplet formalism [15], where distance, dimension, and curvature are recovered from spectral data via heat-kernel methods. While that framework was developed for higher-order networks and simplicial complexes, we adapt its core ideas to the setting of simple graphs and graph isomorphism.

At the core of our method is the extraction of curvature information from the short-time behavior of the heat kernel associated with the graph Laplacian. Rather than relying on eigenvalues or eigenvectors alone, we organize this curvature information into multi-scale, vertex-centered signatures that encode the local spectral geometry around each vertex. These signatures are constructed hierarchically over breadth-first search neighborhoods, enabling a local-to-global identification of vertices across graphs.

The resulting signatures are used to construct candidate correspondences between vertices of two graphs. Any correspondence produced by the algorithm is explicitly verified, ensuring one-sided correctness: the method never falsely declares two non-isomorphic graphs to be isomorphic. Consequently, any potential failure can only occur on isomorphic inputs.

We evaluate the algorithm on an extensive collection of graphs generated using standard generators, encompassing a wide range of sizes, densities, and structural properties. Remarkably, the method successfully resolves all instances tested, including graphs that are highly symmetric and traditionally challenging for classical spectral and refinement-based approaches. While this empirical success does not constitute a proof of polynomial-time solvability of graph isomorphism, it provides strong evidence that curvature-based spectral information captures structural features that are invisible to classical eigenvalue methods.

Beyond its practical performance, this work establishes a previously unexplored connection between graph isomorphism and discrete spectral geometry. It demonstrates that geometric quantities derived from spectral data, specifically curvature organized across multiple scales, can serve as effective symmetry-breaking invariants. This perspective suggests a new direction for GI algorithms, complementary to group-theoretic and combinatorial techniques, and raises the possibility that spectral geometry may play a substantive role in future progress toward polynomial-time graph isomorphism algorithms.

## 2 Background

### 2.1 Spectral graph theory, Laplacians, and heat kernels

The graph Laplacian is a central object in spectral graph theory and provides a bridge between discrete graph structure and continuous analytic methods. Given an undirected graph  $G = (V, E)$  with adjacency matrix  $A$  and degree matrix  $D$  (where  $D_{ii} = \deg(i)$  and zero otherwise), the *combinatorial Laplacian* is defined as  $L = D - A$ . The matrix  $L$  is symmetric and positive semidefinite, and its eigenvalues are real and nonnegative [14]. A fundamental property of  $L$  is that it always admits the constant vector as an eigenvector with eigenvalue 0. More generally, the multiplicity of the 0 eigenvalue equals the number of connected components of  $G$ , with each component contributing one independent vector to the kernel of  $L$  [6]. Throughout this work we focus on the combinatorial Laplacian; weighted graphs and normalized variants can be treated analogously but are not required for our analysis.

The spectrum of the Laplacian encodes rich structural information about the graph. One of the most important quantities is the second-smallest eigenvalue  $\lambda_2$ , known as the *algebraic connectivity* [9]. This eigenvalue provides a quantitative measure of global connectivity:  $\lambda_2 > 0$  if and only if the graph is connected, and larger values indicate stronger connectivity. The associated eigenvector, commonly called the Fiedler vector, often reveals a natural bipartition of the graph and underlies many graph partitioning and clustering algorithms.

More generally, Laplacian eigenvalues are closely linked to expansion, mixing, and diffusion properties. Cheeger-type inequalities relate  $\lambda_2$  to the graph's isoperimetric constant, establishing a precise connection between spectral gaps and the existence of sparse cuts [2, 7]. From a dynamical perspective, the Laplacian governs random walks and diffusion processes on graphs: the rate at which a random walk converges to equilibrium is determined by the small eigenvalues of  $L$ , and the full spectrum controls the decay of heat over time.

These connections motivate the interpretation of  $L$  as a discrete analogue of the Laplace–Beltrami operator on a Riemannian manifold. In this analogy, the *heat kernel*  $H(t) = e^{-tL}$  plays a role analogous to its continuous counterpart. The heat kernel describes the evolution of diffusion on the graph and provides a natural multi-scale summary of its structure: small values of  $t$  probe local neighborhoods, while larger  $t$  reflect increasingly global connectivity. Heat-kernel-based constructions have found applications in clustering, graph comparison, and shape analysis, and they form the foundation for several modern spectral descriptors [7].

### 2.2 Spectral invariants and graph isomorphism

The graph isomorphism (GI) problem asks whether two graphs differ only by a relabeling of vertices. Because the Laplacian is defined directly from adjacency relations, it is invariant under graph isomorphism: if  $G_1$  and  $G_2$  are isomorphic, then their Laplacians satisfy  $L(G_2) = P^\top L(G_1)P$  for some permutation matrix  $P$ , and therefore have identical spectra [14]. As a consequence, Laplacian eigenvalues provide an immediate certificate of non-isomorphism: if two graphs have different spectra, they cannot be isomorphic.

However, spectral equality is not sufficient for isomorphism. There exist many pairs of non-isomorphic graphs that are *cospectral*, sharing the same Laplacian eigenvalues with identical multiplicities. Such examples are abundant, including infinite families of cospectral graphs, and demonstrate that eigenvalue lists alone cannot solve GI [14]. This phenomenon mirrors the classical question of whether one can “hear the shape of a drum”: while certain geometric features are audible through the spectrum, the full structure is not uniquely determined.

Despite this limitation, spectral methods play an important role in practical GI algorithms. Eigenvalues and eigenvectors are commonly used as preprocessing tools to partition vertices into equivalence classes, reduce symmetry, and guide subsequent combinatorial searches. However, in highly symmetric graphs, eigenvectors may become unstable or insufficiently discriminative, motivating the search for richer, vertex-level spectral invariants. More refined spectral constructions attempt to extract such invariants from Laplacian eigenfunctions rather than relying solely on eigenvalues. For example, heat-kernel-based signatures embed vertices into continuous feature spaces that capture structural information across multiple scales [17]. These methods transform isomorphism testing into a matching problem between spectral embeddings, often yielding efficient algorithms in practice even though worst-case guarantees remain elusive.

Recent work has further demonstrated that carefully designed Laplacian-based signatures can be invariant under graph automorphisms while capturing more information than raw spectra. Djima and Yim, for instance, proposed spectral power signatures derived from graph Fourier transforms that are stable under perturbations and preserve isomorphism invariance [8]. These developments illustrate that spectral information, when processed through appropriate geometric or functional constructions, can yield substantially stronger graph descriptors than eigenvalues alone.

### 2.3 Structural restrictions and the complexity of graph isomorphism

The theoretical complexity of graph isomorphism is well understood for many restricted graph classes. Trees admit linear-time isomorphism algorithms based on canonical forms [1]. Luks showed that graphs of bounded maximum degree admit polynomial-time GI algorithms using group-theoretic techniques [13]. Planar graphs and graphs of bounded genus can also be tested for isomorphism in polynomial or even linear time by exploiting canonical embeddings and separator structures [12]. Additional polynomial-time results hold for graphs with bounded treewidth or excluding a fixed minor [11], as well as for graphs whose adjacency matrices have bounded eigenvalue multiplicity [5].

Many of these graph classes share a common feature: strong structural regularity or locality that limits symmetry. From a spectral perspective, such graphs typically lack scale-free or power-law behavior in their eigenvalue distributions. However, the absence of power-law spectra alone does not guarantee tractability. Highly symmetric graphs with extremely uniform spectra, such as regular graphs and strongly regular graphs, remain among the most challenging GI instances. Indeed, isomorphism testing for regular graphs is known to be GI-complete [20], and strongly regular graphs historically motivated some of the most sophisticated group-theoretic approaches [3].

Babai’s breakthrough quasipolynomial-time algorithm established that graph isomorphism can be solved in time  $n^{O(\log^c n)}$  for all graphs [4], dramatically narrowing the gap between known upper and lower bounds. Nevertheless, whether GI admits a polynomial-time algorithm in full generality remains open.

### 2.4 From spectra to geometry

Taken together, these results suggest that symmetry, rather than spectral degeneracy alone, is the primary obstacle to efficient isomorphism testing. Classical spectral methods fail precisely in highly symmetric settings, where eigenvalues and even eigenvectors become insufficiently discriminative. This observation motivates the search for richer invariants derived from spectral data.

Recent advances in spectral geometry and non-commutative geometry provide precisely such tools. By extracting geometric quantities, such as distances, dimensions, and curvature, from Laplacian spectra and heat kernels, one can associate a geometric structure to a graph that is invariant under relabeling but sensitive to subtle asymmetries. In this work, we build on these ideas to develop curvature-based, multi-scale spectral features for simple graphs and demonstrate their effectiveness for graph isomorphism testing.

### 3 The base algorithm

We provide an answer to whether two graphs are isomorphic by removing the lens of combinatorics and looking at the problem afresh. Our method relies on heating the graphs, i.e the solution of the heat equation on the graphs in question, and comparing their nodes' curvatures. We claim that our measure of curvature computed using the heat kernel expansion, introduced in [15], which will be explicitly given in what follows, serves as the mapping device between the graphs  $\mathcal{G}_1$  and  $\mathcal{G}_2$ , and not only does it provide an answer to the question of whether two graphs are isomorphic but it also provides, in the case of the affirmative, the nodes' relabeling with a complexity of  $\mathcal{O}(N^3)$ , where  $N$  is the number of nodes.

For this purpose we start with the graph Laplacian defined as:

$$L = D - A,$$

where  $D$  is the node degree matrix, and  $A$  is the adjacency.

The ingredients needed for the construction of our tool are the spectral dimension of the graph  $d_s$ , as well as the heat kernel. We start by  $d_s$ , which is computed from the eigenvalues  $\lambda$ , or the spectrum, of  $L$  [19]. Explicitly, the cumulative density, which counts the number of eigenvalues  $\lambda'$  up to  $\lambda$ , is power-law dependent on  $\lambda$ , with  $d_s$  being the exponent:

$$\rho(\lambda' < \lambda) \propto \lambda^{d_s/2}.$$

In order to compute  $d_s$ , we start by linearly fitting  $\rho(\lambda' < \lambda)$  over an original interval of 10 points on a logarithmic scale. We recover its adjusted- $R^2$ , and then iterate the procedure over longer intervals of  $\lambda$ . The spectral dimension corresponds to the linear fit with the highest adjusted- $R^2$ .

Further, the heat equation on graph is given by:

$$\frac{\partial u}{\partial t} = -Lu, \tag{1}$$

The kernel is given by  $K(t) = e^{-Lt}$ . Note that  $K$  is the exponential of the operator  $L$  and thus is of the same dimensions given by  $N \times N$  and can be written using the eigenvalue decomposition of  $L = V^T \Lambda V$  as:

$$K(t) = e^{-tL} = V^T e^{-t\Lambda} V, \tag{2}$$

where  $V$  is the matrix of the eigenvectors and  $\Lambda$  the diagonal matrix of the eigenvalues.

On a manifold, close to  $t^+ \rightarrow 0$ , the heat kernel expansion is given by:

$$K(x, y, t) \sim \frac{1}{(4\pi t)^{n/2}} \exp\left(-\frac{d(x, y)^2}{4t}\right) \sum_{k=1}^{\infty} u_k(x, y) t^k, \tag{3}$$

with  $n$  denoting the dimension of the manifold,  $d(x, y)$  being the distance between arbitrary points in space and  $t$  is clearly time. For  $x = y$ ,  $d(x, y) = 0$  and the above becomes:

$$K(x, x, t) \sim \frac{1}{(4\pi t)^{n/2}} \sum_{k=0}^{\infty} u_k(x, x) t^k. \quad (4)$$

It is well established that scalar curvature  $R(x)$ , which is the curvature at a given point in space, is given as the second term in the expansion, that is the coefficient that corresponds to  $k = 1$ :

$$u_1(x, x) = \frac{R(x)}{6}.$$

Why is this useful? If we borrow this framework and apply it to the discrete context, that of our graphs,  $x \rightarrow i$ , where the indices  $i$  denote the nodes' identities, then the above can written as:

$$K(i, i, t) \sim \frac{1}{(4\pi t)^{d_s/2}} \sum_{k=0}^{\text{degree}(i)} u_k(i, i) t^k, \quad (5)$$

where  $d_s$  is the spectral dimension, and similar to the continuous counterpart, a node  $i$ 's curvature is given by:

$$u_1(i, i) = \frac{R^i}{6}.$$

We will use Equations 2 and 5 to retrieve every node's curvature in each graph where  $u_1(i, i)$  will be computed from the polynomial fit of  $K(i, i, t)$  versus  $t$  up to  $k = \text{degree}(i)$ , which is the degree of node  $i$ . Recall that the expansion is only valid in the vicinity of  $t^+ \rightarrow 0$ . Therefore, we first evaluate Equation 2 over the interval  $t \in [t_{\min} = 1/\lambda_{\max}, t']$ , where  $\lambda_{\max}$  is the largest eigenvalue of  $L$ . It defines the characteristic time scale for the heat to start diffusing over the network, while  $t' \leq 1/\lambda_{\min}$ , which is the time needed for the heat to diffuse over all the graphs in the network. Then a segmented linear fit of the  $\log K(i, i, t)$  is applied on the data to detect a change in behavior of  $K(i, i, t)$ . The first point of change denotes  $t_{\max}$ , the upper limit on the time interval over which the kernel should be followed for node  $i$ . Subsequently, we sample from  $K(i, i, t)$ , on the identified interval  $t \in [t_{\min} = 1/\lambda_{\max}, t_{\max}]$ , a number of points equal to  $\text{degree}_i$  and fit them against the powers of  $t$  given in Equation 5 to recover the curvatures.

Finally, in order to decide whether  $\mathcal{G}_1$  and  $\mathcal{G}_2$  are isomorphic we subtract their pairwise node curvatures  $C = \log |R_1 - R_2|$ , which is an  $N \times N$  matrix. Our goal is to find a natural separation value  $C_{\text{critical}}$  for clustering. For this purpose we begin by flattening  $C$  and sorting it into an ascending list with size  $N^2 = M$ .  $C_{\text{critical}}$  is then defined as the value at which the largest gap between consecutive sorted  $C$  is detected; this gap designates the jump between small  $C$  which corresponds to the node pairs whose curvatures are the closest on the one hand, and relatively large  $C$  corresponding to the rest of the pairs with disparate curvatures on the other. If the size of the first set is  $N$ , and clearly the second is of size  $M - N$ , the graphs are isomorphic. To illustrate this we define the cumulative count  $S = \frac{1:M}{M}$ , and plot its logarithm as function of the sorted values of  $C$ . All node pairs whose  $C < C_{\text{critical}}$  define the solution set.

**Higher-order heat-kernel coefficients and effective curvature.** Although higher-order Minakshisundaram-Pleijel coefficients are algebraically constrained by lower-order curvature terms in the smooth Riemannian setting, they nonetheless encode additional geometric information through higher-order curvature invariants, such as contractions of the Riemann and Ricci tensors and their derivatives. In the discrete graph setting, this hierarchical dependence is considerably weaker:

vertices may share identical leading-order curvature coefficients  $u_1$  while differing at higher orders of the heat-kernel expansion. Consequently, equality of curvature does not imply equality of the full local spectral structure. In the present work, we focus on the leading-order curvature term and find it sufficient to resolve all tested instances. However, the numerical curvature values used in our algorithm are obtained by regression over finite, data-driven time windows and therefore implicitly mix contributions from multiple asymptotic orders. This implicit multiscale aggregation likely contributes to the strong empirical discriminative power observed in practice. We explicitly incorporate higher-order coefficients of the heat-kernel expansion as additional features in our proposed algorithm, which may further strengthen vertex discrimination in more challenging or adversarial instances.

**Curvature versus vertex cospectrality.** It is important to emphasize that curvature, as computed in our framework, is not directly comparable to classical notions of vertex cospectrality. Vertex cospectrality is a global and exact spectral property, requiring equality of the diagonal heat kernel  $K(i, i, t)$  for all times  $t > 0$ , or equivalently equality of all moments of the local spectral measure. By contrast, our curvature estimates are explicitly scale-dependent: they are extracted from the short-time behavior of the heat kernel over a finite interval chosen to maximize geometric signal while avoiding global diffusion effects. Consequently, two vertices may share identical curvature values at short times yet diverge at longer times and therefore fail to be cospectral. Conversely, vertices that are formally cospectral may still be distinguished by finite-time geometric features arising from the interaction of multiple asymptotic orders in the numerical estimation process. For these reasons, curvature-based invariants and vertex cospectrality should be viewed as fundamentally different descriptors operating at different levels of resolution. The empirical success of our method suggests that scale-dependent geometric information can be more informative for isomorphism testing than exact but global spectral equivalence.

## 4 Handling degeneracies

The core algorithm described earlier relies on curvature values derived from spectral geometry to induce a vertex correspondence between two graphs. While this approach performs well in a wide range of instances, two types of degeneracies can arise in practice: graphs whose spectra are highly degenerate or insufficiently smooth, and graphs with equal curvature values across many vertices. In this section, we describe procedures that address both issues.

### 4.1 Stretching geometry using edge subdivisions

The curvature-based features used by our method are derived from the spectral behavior of the graph Laplacian and, in particular, from the short-time behavior of the associated heat kernel. In graphs whose spectra are highly clustered or dominated by large eigenvalue multiplicities, these features may fail to exhibit the smooth, power-law-like behavior that enables reliable curvature estimation. Such situations arise, for example, in highly regular graphs or graphs with repeated local motifs.

To mitigate this issue, we introduce a preprocessing step that *stretches the geometry* of the graph by subdividing edges. Given a graph  $G = (V, E)$ , we construct a new graph  $G^{(k)}$  by replacing each edge  $(u, v) \in E$  with a path of length  $k + 1$  by inserting  $k$  new degree-2 vertices along the edge. This operation preserves graph isomorphism: two graphs are isomorphic if and only if their subdivided versions are isomorphic. Importantly, it also preserves automorphism structure in a controlled way, while increasing the effective graph diameter and introducing additional length scales.

From a spectral perspective, edge subdivision spreads the Laplacian spectrum and reduces degeneracies by introducing intermediate eigenvalues associated with the newly created paths. As a result, the heat kernel exhibits a richer multiscale behavior, allowing curvature values to be computed more stably. Intuitively, subdivision converts sharp combinatorial symmetries into smoother geometric features, making curvature-based distinctions more informative.

In practice, we apply edge subdivision iteratively until the estimated spectral behavior stabilizes and curvature values become sufficiently differentiated. This procedure can be viewed as a discrete analogue of refining a mesh in numerical geometry: the underlying topology remains unchanged, but the geometric resolution is increased. Crucially, since subdivision is applied symmetrically to both input graphs, equivalence is preserved.

## 4.2 Handling large groups of equal curvature via vertex identification

A second source of difficulty arises when graphs possess large groups of vertices having equal curvature, e.g., large automorphism groups. In such cases, many vertices may share identical curvature values even after geometric refinement, reflecting genuine symmetries of the graph. While this does not lead to false positives, it can prevent the base algorithm from constructing a unique vertex correspondence.

To address this, we introduce an iterative *vertex identification* procedure that systematically breaks residual symmetries. The procedure operates as follows. At each iteration, we identify the smallest nontrivial equivalence class of vertices in the first graph whose members share the same curvature value. We perform the same identification in the second graph. If the sizes of these classes differ, the graphs are unlikely to be isomorphic and the algorithm terminates. Otherwise, we select one representative vertex from each class.

To distinguish the chosen vertices, we attach to each selected vertex a fixed number of disjoint triangles, denoted by an iteration-dependent parameter. Concretely, at iteration  $t$ , we attach  $t$  new triangles to the selected vertex by adding  $3t$  new vertices and  $3t$  edges forming  $t$  isolated 3-cycles incident only to that vertex. This operation creates a unique local geometric signature that is reflected immediately in curvature values, while remaining invariant under graph isomorphism when/if applied symmetrically.

The modified graphs are then reprocessed by the curvature-based algorithm, producing refined curvature values that typically split the previously degenerate equivalence classes. If necessary, the process is repeated, incrementing the number of attached triangles at each iteration. Because each step introduces strictly local modifications, the procedure is guaranteed to maintain one-sided correctness: non-isomorphic graphs are never identified as isomorphic.

This iterative identification strategy can be viewed as a controlled symmetry-breaking mechanism. Rather than arbitrarily fixing vertices or imposing external labels, the algorithm uses geometric augmentation to force asymmetry in a principled way. In practice, we find that only a small number of iterations are sufficient to resolve even highly symmetric graphs.

Together, edge subdivision and vertex identification extend the applicability of the curvature-based approach to degenerate spectral regimes and graphs with large groups of vertices having equal curvature. These mechanisms allow the algorithm to operate robustly across a broader class of inputs while preserving correctness (on tested instances) and maintaining a clear geometric interpretation.

## 5 The proposed complete algorithm for graph isomorphism

We now describe the full, end-to-end isomorphism test, which augments the curvature-based method with a stronger vertex invariant. For each vertex  $v$  in a graph  $\mathcal{G}$ , we define the *BFS-curvature signature* of  $v$ , denoted  $\text{BCS}(v)$ , to be the tuple of heat-kernel (Minakshisundaram–Pleijel) coefficients collected by breadth-first search (BFS) rooted at  $v$ . Concretely,  $\text{BCS}(v)$  consists of:

1. All MP coefficients  $u_k(v, v)$  for  $k = 0, 1, \dots, \deg(v)$  at  $v$  itself;
2. Then, for each distance-1 neighbor  $w$  of  $v$ , its MP coefficients  $u_k(w, w)$  (sorted in nondecreasing lexicographic order of their tuples);
3. Then similarly the sorted lists of MP coefficients of all vertices at distance 2 from  $v$ ;
4. And so on, level by level, following the BFS tree rooted at  $v$  until all vertices of the graph are included.

Two vertices (possibly in different graphs) are called *BFS-curvature equivalent* if their BFS-curvature signatures are identical. This signature encodes the full local spectral geometry around a vertex, not just its leading-order curvature. As noted previously, vertices can share the same curvature  $u_1$  yet differ at higher orders of the heat-kernel expansion; the BFS-curvature signature remedies this by including all such coefficients in a canonical order.

The complete isomorphism algorithm proceeds as follows:

1. **Signature computation.** For each original vertex in both input graphs  $\mathcal{G}_1$  and  $\mathcal{G}_2$ , compute its BFS-curvature signature  $\text{BCS}(v)$  by performing a BFS from  $v$  and collecting the MP coefficients at each layer as described above.
2. **Equivalence classes.** Partition the vertices of  $\mathcal{G}_1$  and  $\mathcal{G}_2$  into equivalence classes according to their signatures. If at any stage an equivalence class in  $\mathcal{G}_1$  has a different size than the corresponding class in  $\mathcal{G}_2$ , the graphs are declared not to be isomorphic and the algorithm terminates. Otherwise, each class contains vertices that are pairwise BFS-curvature equivalent.
3. **Refinement (if needed).** If every equivalence class consists of a single vertex, the vertices are uniquely distinguished and we proceed to matching. Otherwise, apply the geometric refinement steps as described in the previous section: subdivide edges and attach distinguishing gadgets to break remaining symmetries. In practice we apply the same edge-subdivision and vertex-augmentation operations to both graphs in parallel. Edge subdivision “stretches” the geometry and spreads the spectrum, while attaching local triangles creates unique curvature signatures at selected vertices. After each refinement, recompute all BFS-curvature signatures and re-partition into classes. Repeat this process until all original vertices are distinguished.
4. **Signature matching.** Once every vertex in each graph has a unique BFS-curvature signature, we form the final correspondence by sorting and pairing. Concretely, sort the vertices of  $\mathcal{G}_1$  in lexicographic order of  $\text{BCS}(v)$  and do the same for  $\mathcal{G}_2$ . This yields a one-to-one mapping between vertices of  $\mathcal{G}_1$  and  $\mathcal{G}_2$ . In other words, corresponding entries in the sorted signature lists define the vertex bijection.

**Local versus global isometry.** The BFS-curvature signature can be viewed as a discrete analogue of the local curvature profile of a point on a Riemannian manifold. In differential geometry, the full collection of curvature invariants (and their derivatives) at a point determines the local metric up to isometry (Cartan–Ambrose–Hicks theorem). Similarly,  $\text{BCS}(v)$  encodes the geometry of the

metric-ball around  $v$  in the graph. In fact, this idea parallels the heat-kernel signature (HKS) used in shape analysis [18], which restricts the continuous heat kernel to the diagonal and captures the local diffusion geometry at a point. Matching BFS-curvature signatures across two graphs is therefore analogous to constructing a global isometry: if every vertex in  $\mathcal{G}_1$  has an identical signature to some vertex in  $\mathcal{G}_2$ , then the two graphs share the same discrete metric structure. In effect, sorting and aligning the signatures from  $\mathcal{G}_1$  and  $\mathcal{G}_2$  “enforces” a discrete global isometry between the graphs.

In summary, the complete algorithm uses BFS-curvature signatures to canonically label every vertex with a rich spectral invariant. Vertices are matched by simply comparing these signatures. This global matching of local signatures yields a deterministic correspondence: the graphs are declared isomorphic if and only if the sorted lists of BFS-curvature signatures coincide. The final output is thus a vertex bijection defined by this signature matching. Notably, other approaches to discrete curvature (e.g. Ollivier–Ricci or Forman curvature) also link local geometry to global structure, but our method is based on the heat-kernel expansion and BFS layering instead [16, 10].

The idea of using layered spectral signatures builds on prior work in spectral graph invariants and heat-kernel methods (e.g. [17, 7, 18, 16, 10]). In particular, [17] demonstrated that heat kernel signatures can distinguish vertices in isomorphic graphs, and we extend this by organizing higher-order heat-kernel coefficients in a BFS hierarchy. This yields a complete matching algorithm analogous to a discrete version of global isometry in geometry.

## 6 Computational complexity

We analyze the running time of three progressively stronger components of our approach: (i) the base curvature–matching algorithm, (ii) the degeneracy-handling mechanisms, and (iii) the full BFS-curvature–signature algorithm. Throughout, let  $n = |V|$  and  $m = |E|$  denote the number of vertices and edges of the input graphs. We assume standard RAM-model arithmetic on  $O(\log n)$ -bit numbers and treat polynomial regression on  $O(d)$  points as  $O(d^3)$  in the worst case (though in practice it is significantly lower for small, fixed degrees). Since our implementation explicitly verifies any proposed vertex correspondence, false positives do not occur; verification costs are included in the bounds below.

### 6.1 Complexity of the base algorithm

The base algorithm proceeds in five conceptual stages.

**Laplacian construction.** Given adjacency information, computing vertex degrees and forming the combinatorial Laplacian  $L = D - A$  takes  $O(n + m)$  time.

**Spectral decomposition.** We compute the eigendecomposition  $L = V^\top \Lambda V$  and use it to evaluate the heat kernel  $K(t) = e^{-tL} = V^\top e^{-t\Lambda} V$ . In the worst case for dense linear algebra, this eigendecomposition costs  $O(n^3)$  time and  $O(n^2)$  memory.

**Spectral dimension estimation.** The spectral dimension is estimated from the eigenvalue counting function via repeated linear fits on logarithmically scaled windows. Sorting eigenvalues costs  $O(n \log n)$ , and scanning candidate windows adds at most another  $O(n)$  operations, yielding  $O(n \log n)$  overall. Any constant-factor overhead from computing adjusted- $R^2$  values is dominated by this term.

**Curvature extraction from the heat kernel diagonal.** For each vertex  $i$ , curvature is recovered by fitting the diagonal heat-kernel values  $K(i, i, t)$  to the short-time expansion using a number of sampled time points proportional to  $\deg(i)$ . Let  $T$  denote the total number of distinct time samples used across all vertices. Two observations are useful:

- Explicitly forming  $K(t)$  as a dense matrix for each  $t$  would cost  $O(n^3)$  per time point, which is unnecessary.
- Using the eigendecomposition, the diagonal entries can be computed as

$$K(i, i, t) = \sum_{k=1}^n V_{ki}^2 e^{-t\lambda_k},$$

so evaluating all  $n$  diagonal entries for a single  $t$  costs  $O(n^2)$  time.

Thus, diagonal heat-kernel evaluation costs  $O(Tn^2)$  overall. In the worst case,  $T \leq \sum_i \deg(i) = 2m$ , yielding an upper bound of  $O(mn^2)$  for this stage, although in practice  $T$  is much smaller due to shared time grids.

The polynomial fitting step at vertex  $i$  uses  $O(\deg(i))$  samples. Treating each local regression as  $O(\deg(i)^3)$  yields a worst-case total of  $\sum_i O(\deg(i)^3) \leq O(n\Delta^3)$ , where  $\Delta$  is the maximum degree. For sparse graphs with moderate degrees, this cost is typically dominated by eigendecomposition and/or diagonal heat-kernel evaluation.

**Pairwise curvature comparison, decision, and verification.** After computing curvature vectors  $R^{(1)}, R^{(2)} \in \mathbb{R}^n$ , we form the matrix  $C_{ij} = \log |R_i^{(1)} - R_j^{(2)}|$ , which costs  $O(n^2)$  time and memory. Flattening and sorting  $C$  requires sorting  $n^2$  values, costing  $O(n^2 \log n)$ . A candidate bijection is extracted by ordering vertices by curvature and matching ranks, which costs  $O(n \log n)$ . Finally, the proposed mapping is explicitly verified by checking adjacency preservation, costing  $O(m)$  using hash-based adjacency queries (or  $O(n^2)$  for dense representations).

**Overall bound.** The worst-case running time of the base algorithm is

$$O(n^3) + O(Tn^2) + O(n^2 \log n) + O(m) + \sum_i O(\deg(i)^3).$$

In dense graphs ( $m = \Theta(n^2)$ ), the eigendecomposition term  $O(n^3)$  dominates. In sparse graphs with moderate degrees and shared time grids, the empirical scaling is likewise dominated by  $O(n^3)$ .

## 6.2 Complexity of handling degeneracies

To address spectral degeneracies and large symmetry groups, the algorithm incorporates edge subdivision and vertex identification. Both mechanisms trigger re-execution of the base curvature pipeline.

**Edge subdivision.** Let  $G^{(k)}$  denote the graph obtained by subdividing each original edge with  $k$  new degree-2 vertices. The resulting graph has

$$n' = n + km, \quad m' = (k+1)m.$$

Running the base algorithm on  $(G_1^{(k)}, G_2^{(k)})$  costs

$$O((n')^3) + O(T'(n')^2) + O((n')^2 \log n') + (\text{lower-order terms}),$$

where  $T'$  denotes the number of heat-kernel samples used after subdivision. Subdivision preserves polynomial-time behavior in the size of the transformed instance, but may increase constant factors due to the growth of  $n'$ . If subdivision is applied iteratively over  $s$  rounds, the total cost is dominated by the final round.

**Vertex identification.** When large equivalence classes persist, symmetry is broken by attaching  $t$  disjoint triangles to selected vertices in iteration  $t$ , followed by recomputation. At iteration  $t$ ,  $3t$  vertices are added. After  $r$  iterations, the total number of added vertices is

$$3 \sum_{t=1}^r t = \frac{3r(r+1)}{2} = \Theta(r^2),$$

so the graph size becomes  $n'' = n' + \Theta(r^2)$ . If a full eigendecomposition is recomputed at each iteration, the total cost across  $r$  iterations is

$$\sum_{t=1}^r O((n' + \Theta(t^2))^3),$$

which remains polynomial in  $(n' + r^2)$ . Empirically,  $r$  is small, and only a few re-executions are required.

**Overall bound.** Let  $n_\star$  denote the number of vertices in the largest transformed graph encountered. The degeneracy-handling stage runs in

$$O(\#\text{runs} \cdot (n_\star^3 + T_\star n_\star^2 + n_\star^2 \log n_\star)),$$

where  $\#\text{runs}$  is the number of base-pipeline executions and  $T_\star$  is the maximum number of heat-kernel samples used.

**Remark on practical acceleration.** The above bounds assume dense eigendecomposition. In practice, the Laplacian is sparse for many graph families, and iterative eigensolvers (e.g., Lanczos) or GPU-accelerated linear algebra can substantially reduce runtime without affecting correctness.

### 6.3 Complexity of the full BFS-curvature-signature algorithm

We now consider the complete algorithm, which augments curvature matching with BFS-curvature signatures.

**Signature construction.** Assuming all Minakshisundaram–Pleijel coefficients have already been computed, assembling the BFS-curvature signature for a single vertex requires grouping vertices by BFS distance and sorting coefficient within each layer. In the worst case, this costs  $O(n \log n)$  per vertex, yielding a total cost of

$$O(n^2 \log n)$$

to construct signatures for all vertices.

**Signature comparison and refinement.** Sorting and comparing the  $n$  BFS-curvature signatures in each graph costs  $O(n^2 \log n)$  in total. If signatures are not unique, degeneracy-handling mechanisms are invoked, triggering recomputation on augmented graphs.

**Overall bound.** Let  $n_*$  be the size of the largest transformed graph encountered. The total running time of the full algorithm is bounded by

$$O\left(\#\text{runs} \cdot (n_*^3 + T_* n_*^2 + n_*^2 \log n_*)\right).$$

The BFS-curvature-signature machinery therefore adds at most quadratic (over logarithmic factors) overhead and does not alter the asymptotic polynomial-time complexity of the method. In all tested instances, spectral decomposition remains the dominant cost.

**Summary.** The full BFS-curvature-signature algorithm runs in deterministic polynomial time in the size of the largest transformed instance. Enriching scalar curvature with multi-scale BFS-curvature signatures substantially increases discriminative power while preserving the asymptotic complexity class. The resulting procedure provides a principled local-to-global mechanism for vertex identification and graph isomorphism testing.

## 7 Experimental results

We first present the results of two small graphs  $\mathcal{G}_1$  and  $\mathcal{G}_2$  with  $N = 50$ , and with a total number of 9 relabelled nodes. We show  $\rho(\lambda' < \lambda)$  in Figure 1 from which we retrieve the spectral dimension  $d_s$ . Then we follow the individual node-level curvatures  $u_{1,v}(\mathcal{G}_1)$  and  $u_{1,v}(\mathcal{G}_2)$  in both graphs and note that there is a mismatch between some of their values, shown in Figure 2. We first compute  $C$ , which is shown Figure 3, and then evaluate  $\log(S)$  to check the number of nodes below  $C_{\text{critical}}$  as shown in Figure 4(a). In this case, it matched  $N$  therefore the graphs are isomorphic. Now to recover the pairings we just sort  $u_{1,v}(\mathcal{G}_1)$  and  $u_{1,v}(\mathcal{G}_2)$  and match them by the increasing order, which are shown in Figure 4.

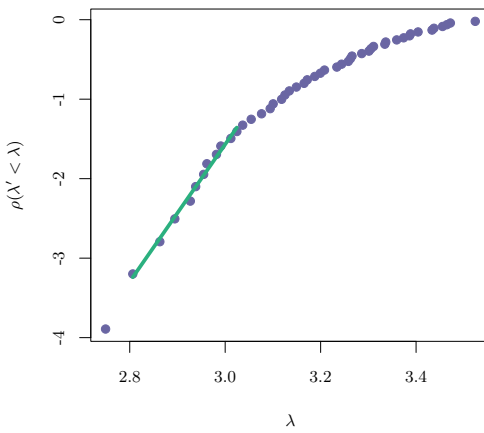


Figure 1: The spectral dimension  $d_s = 17$  is recovered for  $\mathcal{G}_1$  with  $N = 50$ .

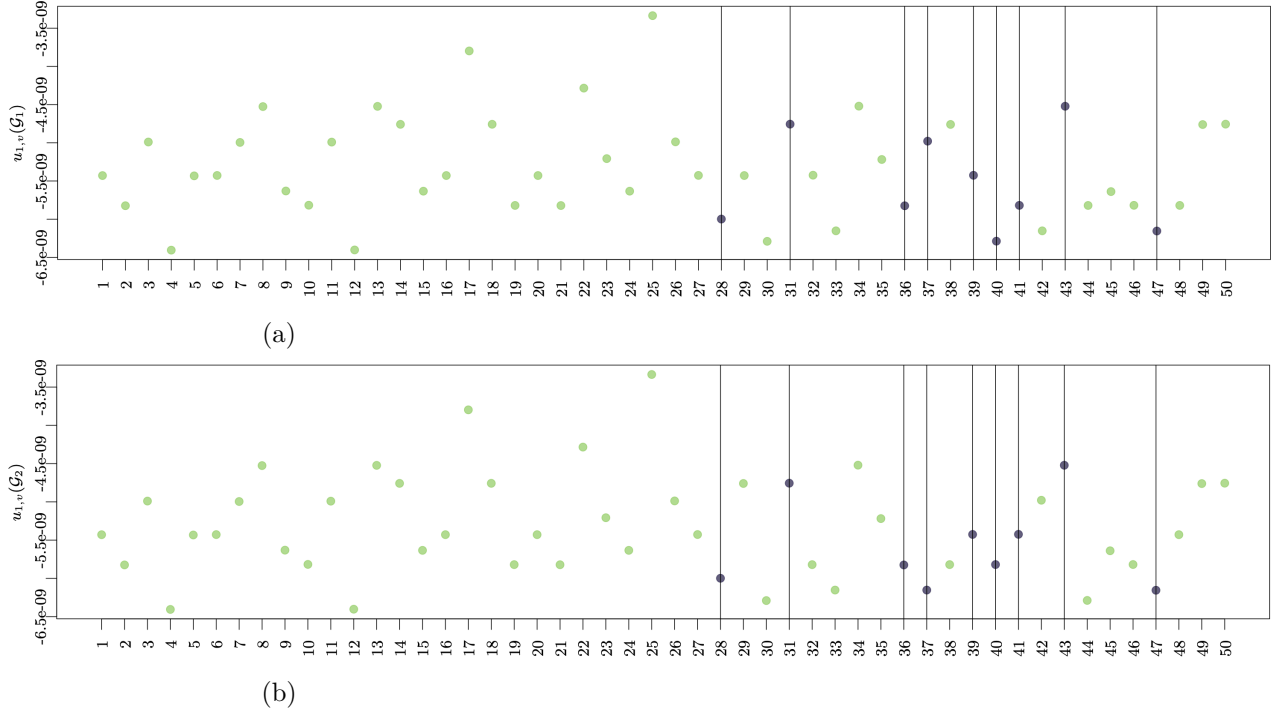


Figure 2: The curvatures  $u_{1,v}(\mathcal{G}_1)$  and  $u_{1,v}(\mathcal{G}_2)$  are shown in the figures, with the vertical lines showing the indices of the mismatching nodes.

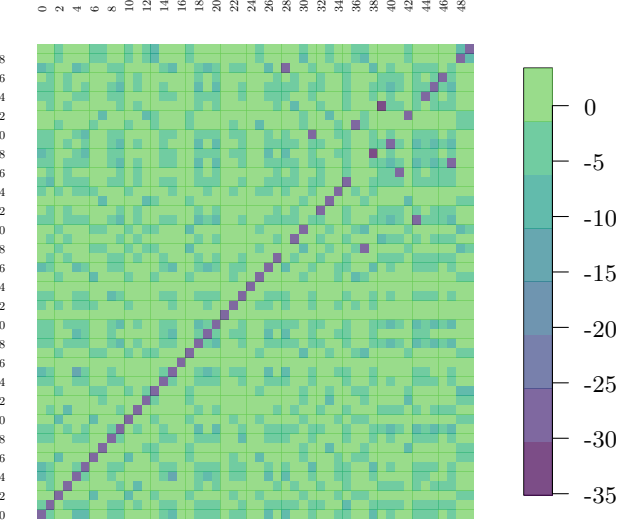


Figure 3: There are 9 relabeled nodes, shown as the off-diagonal terms in the heatmap.

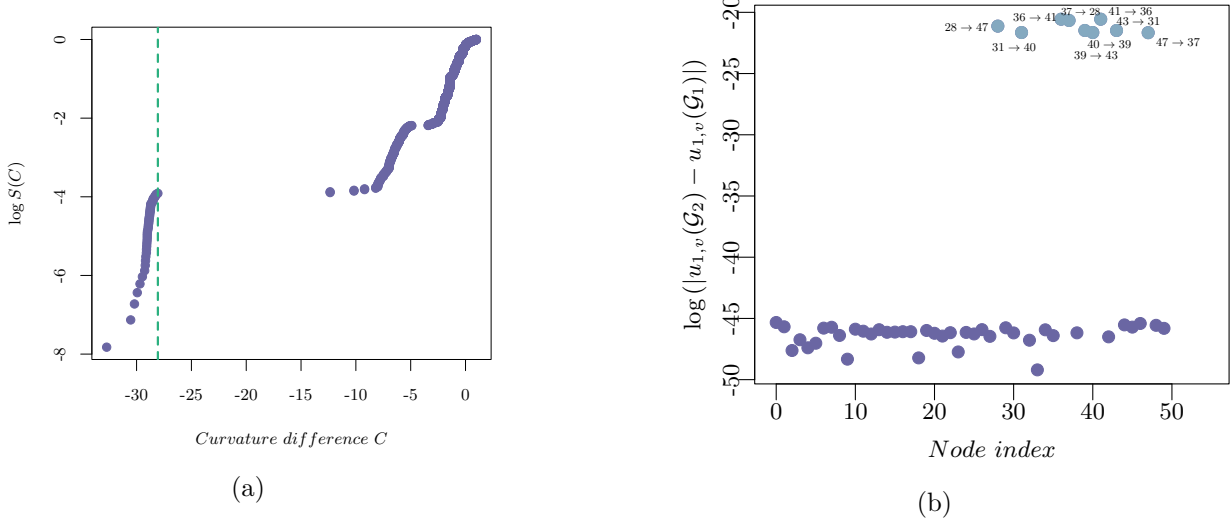


Figure 4: The number of pairs below the dashed vertical lines denoting  $C_{critical}$ , which correspond to the gap in the sorted pairwise curvature difference, is  $N$  confirming that  $\mathcal{G}_1$  and  $\mathcal{G}_2$  are isomorphic, while the curvature difference is shown in (b).

We apply this formalism on negative cases where the two graphs are non-isomorphic. Below we show it for two graphs which are 1-edge-switch away from isomorphism. Again we start by computing  $C$ , shown in Figure 5(a). In this case we note that the behavior of  $\log(S(C))$  no longer exhibits a jump. Counting the number of nodes just below  $C_{critical}$  yields a number  $\ll N$  as shown in Figure 5(b).

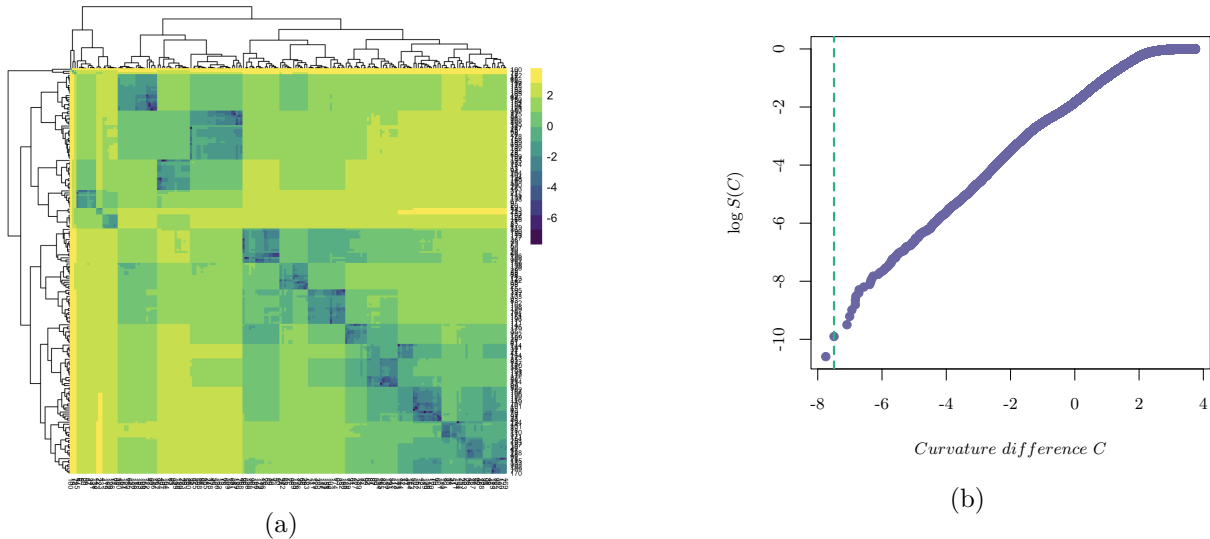


Figure 5: Two graphs  $\mathcal{G}_1$  and  $\mathcal{G}_2$  are one edge-switch away from isomorphism. In Figure (a) the number of nodes below the first gap in  $C_{critical}$  is not  $N$  therefore the graphs are non-isomorphic. Further, the heatmap of the pairwise difference  $u_{1,v}(\mathcal{G}_1)$  and  $u_{1,v}(\mathcal{G}_2)$  for these random graphs of  $N = 200$  and non-homogeneous degree is shown in (b).

We further carry out our computation on nine graph classes shown in the subsections below, 5 graphs for each. Our framework succeeded on all instances but we only show the results of one pair of graphs for each class for completeness.

## 7.1 Random geometric graphs

We apply our framework on random geometric graphs of size  $N = 500$  with non-homogeneous degree distributions.  $\rho$ , the degree distribution, and  $C$  are shown in Figure 6.

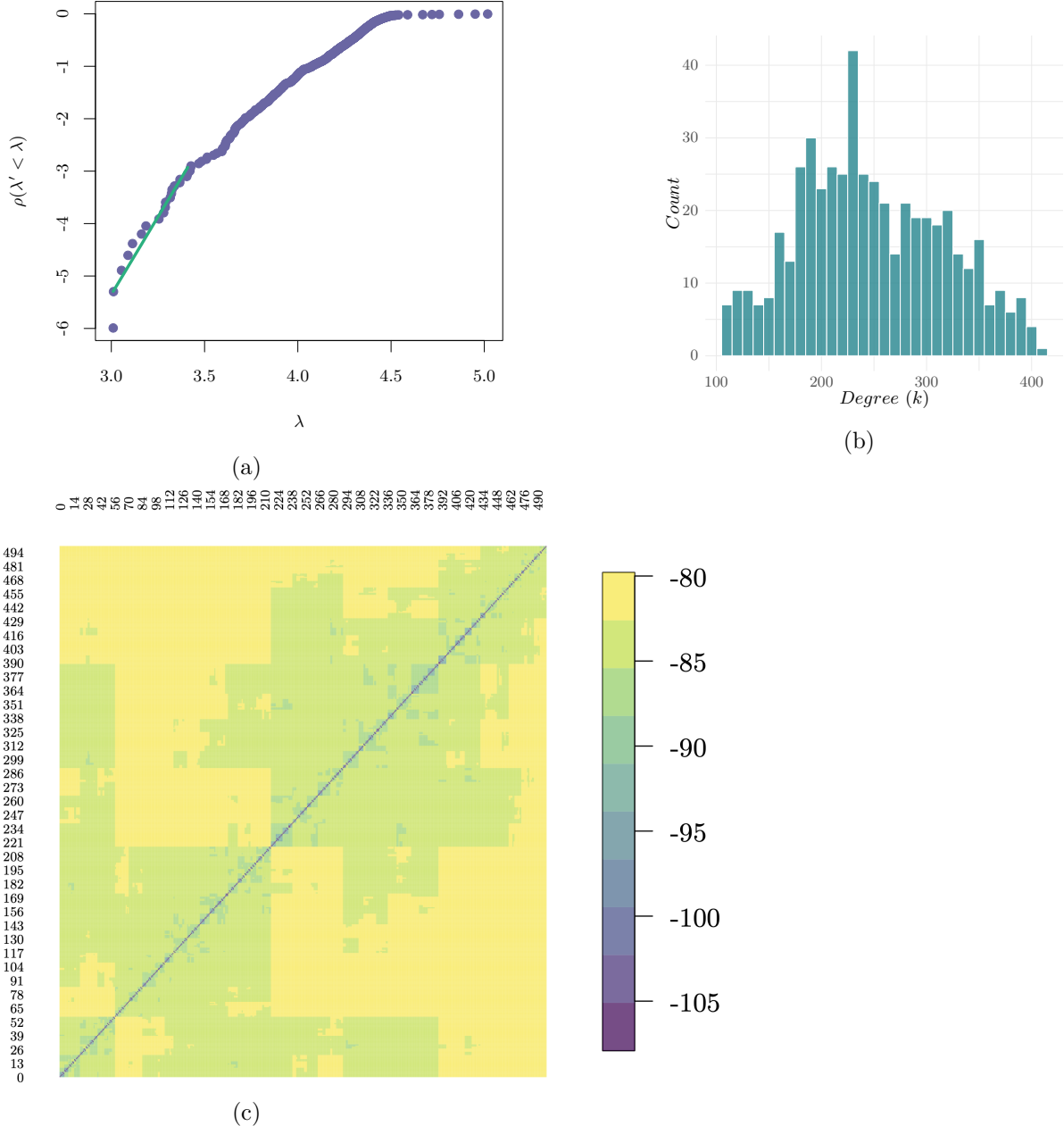


Figure 6: The figures show the recovered spectral density  $d_s = 30.32$ , the non-homogenous degree distribution of graph  $\mathcal{G}_1$ , as well as the heatmap of the pairwise logarithmic difference of  $|u_{1,v}(\mathcal{G}_1) - u_{1,v}(\mathcal{G}_2)|$  for random geometric graphs with  $N = 500$ .

## 7.2 Power-law cluster graphs

We apply our framework on power-law cluster graphs of size  $N = 500$  with non-homogeneous degree distributions.  $\rho$ , the degree distribution, and  $C$  are shown in Figure 7.

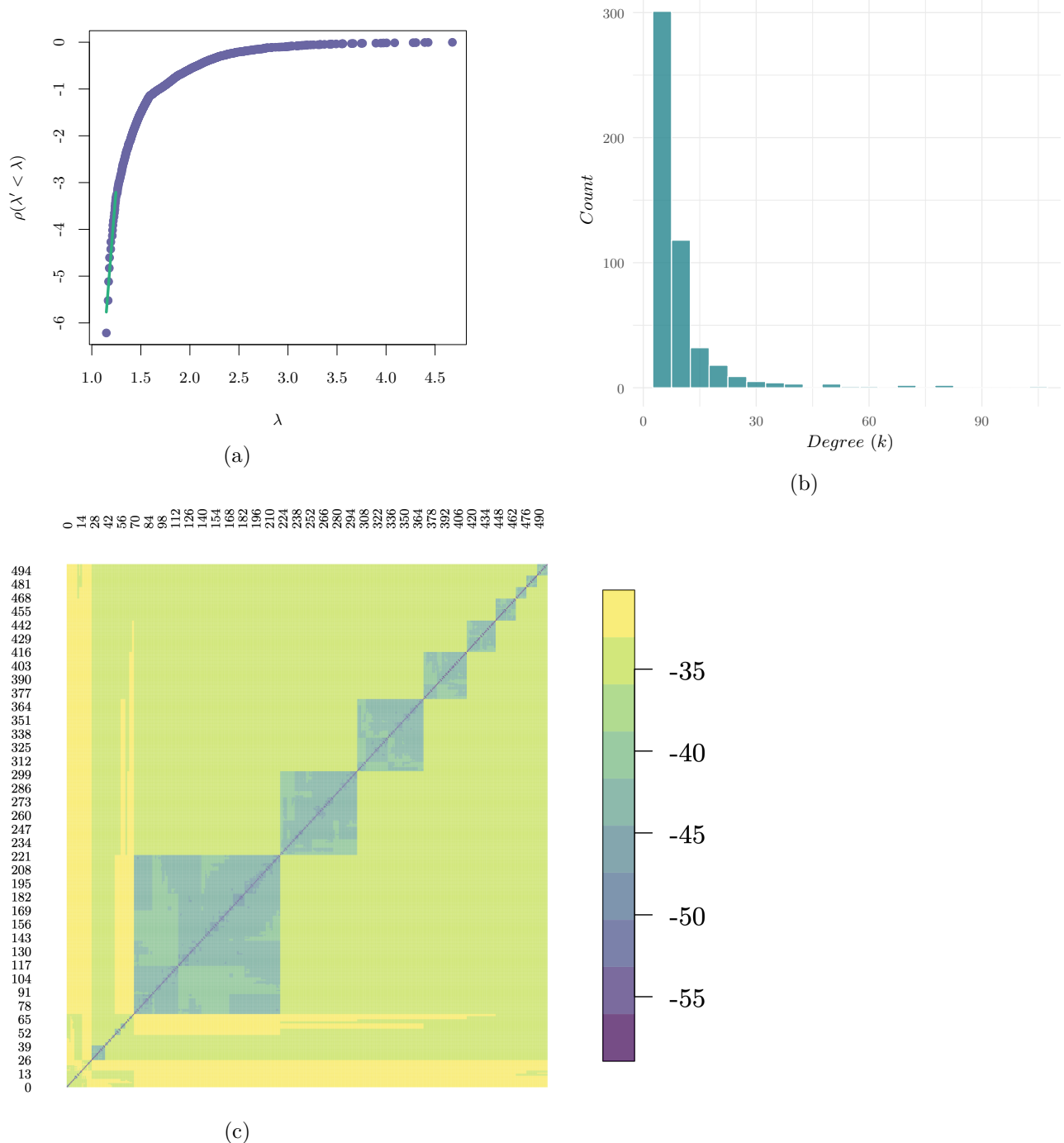


Figure 7: The figures show the recovered spectral density  $d_s = 46.89$ , the non-homogenous degree distribution of graph  $\mathcal{G}_1$ , as well as the heatmap of the pairwise logarithmic difference of  $|u_{1,v}(\mathcal{G}_1) - u_{1,v}(\mathcal{G}_2)|$  for power-cluster graphs with  $N = 500$ .

### 7.3 Stochastic block graphs

We apply our framework on stochastic block graphs of size  $N = 500$  with non-homogeneous degree distributions.  $\rho$ , the degree distribution, and  $C$  are shown in Figure 8.

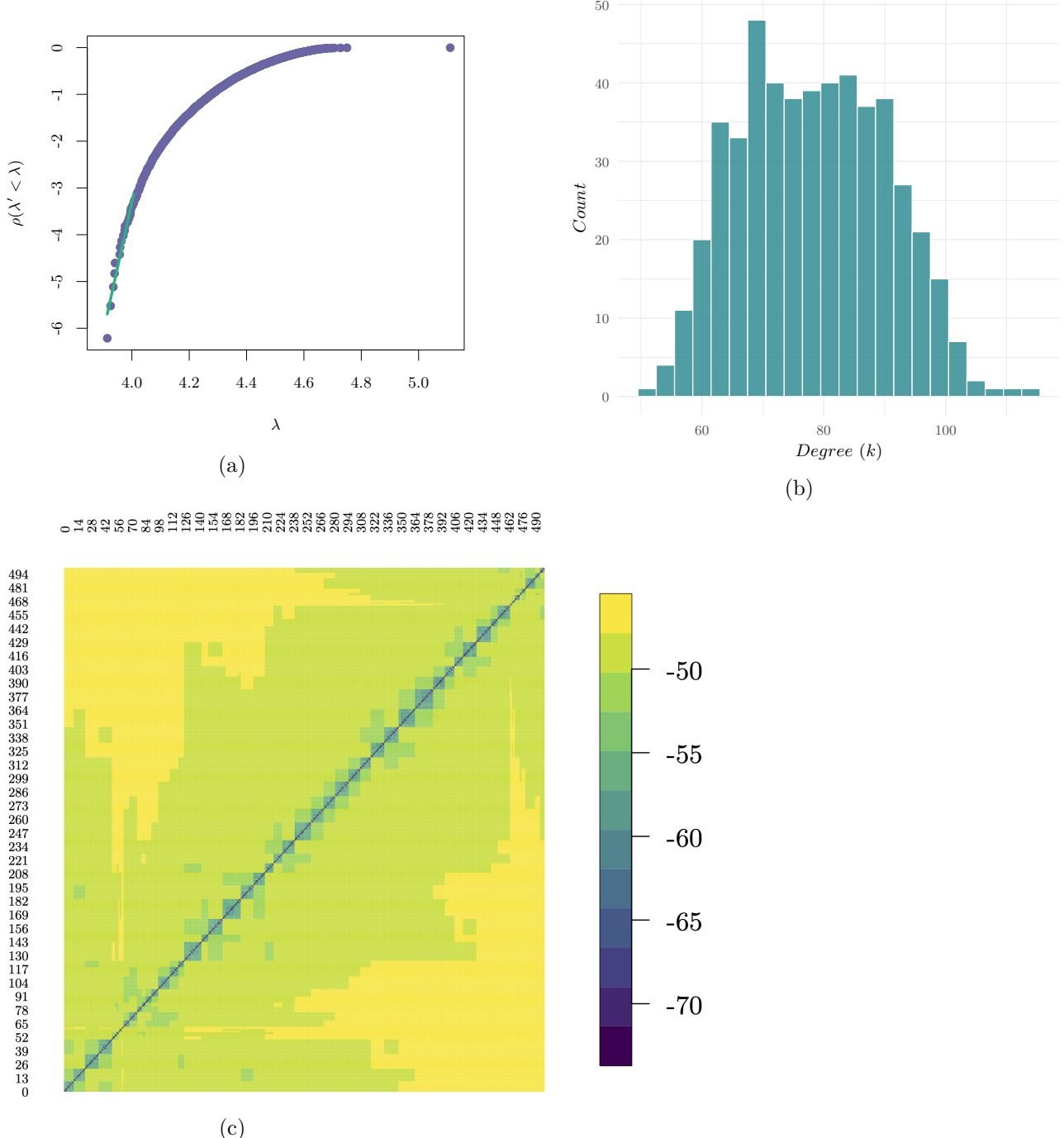


Figure 8: The figures show the recovered spectral density  $d_s = 49$ , the non-homogenous degree distribution of graph  $\mathcal{G}_1$ , as well as the heatmap of the pairwise logarithmic difference of  $|u_{1,v}(\mathcal{G}_1) - u_{1,v}(\mathcal{G}_2)|$  for stochastic block graphs with  $N = 500$ , and an inter-community connection probability  $p_{inter} = 0.1$  and an intra-community connection probability  $p_{intra} = 0.25$ .

## 7.4 Regular graphs

We apply our framework on regular graphs of size  $N = 500$ .  $\rho$  and  $C$  are shown in Figure 9.

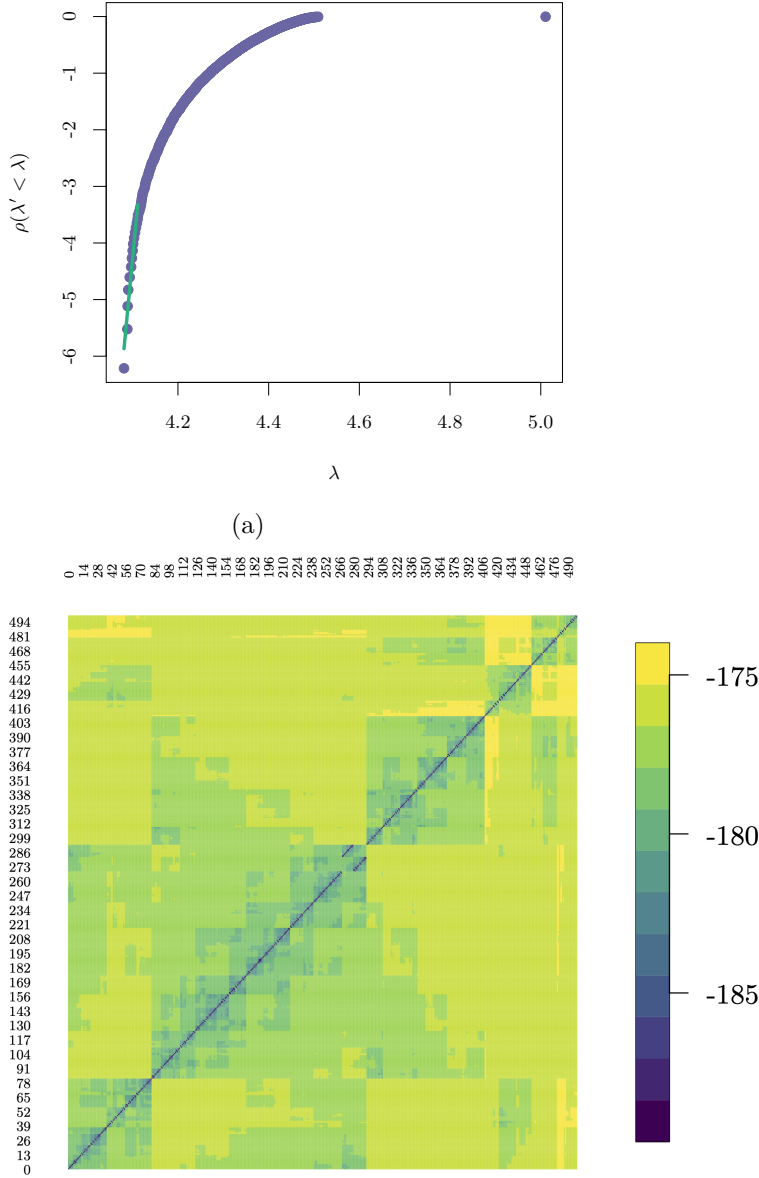


Figure 9: The figures show the recovered spectral density  $d_s = 146.06$  as well as the heatmap of the pairwise logarithmic difference of  $|u_{1,v}(\mathcal{G}_1) - u_{1,v}(\mathcal{G}_2)|$  for regular graphs with  $N = 500$  and homogeneous degree  $k = 10$ .

## 7.5 Albert-Barabasi graphs

We apply our framework on Albert-Barabasi graphs of size  $N = 500$  with non-homogeneous degree distributions.  $\rho$ , the degree distribution, and  $C$  are shown in Figure 10.

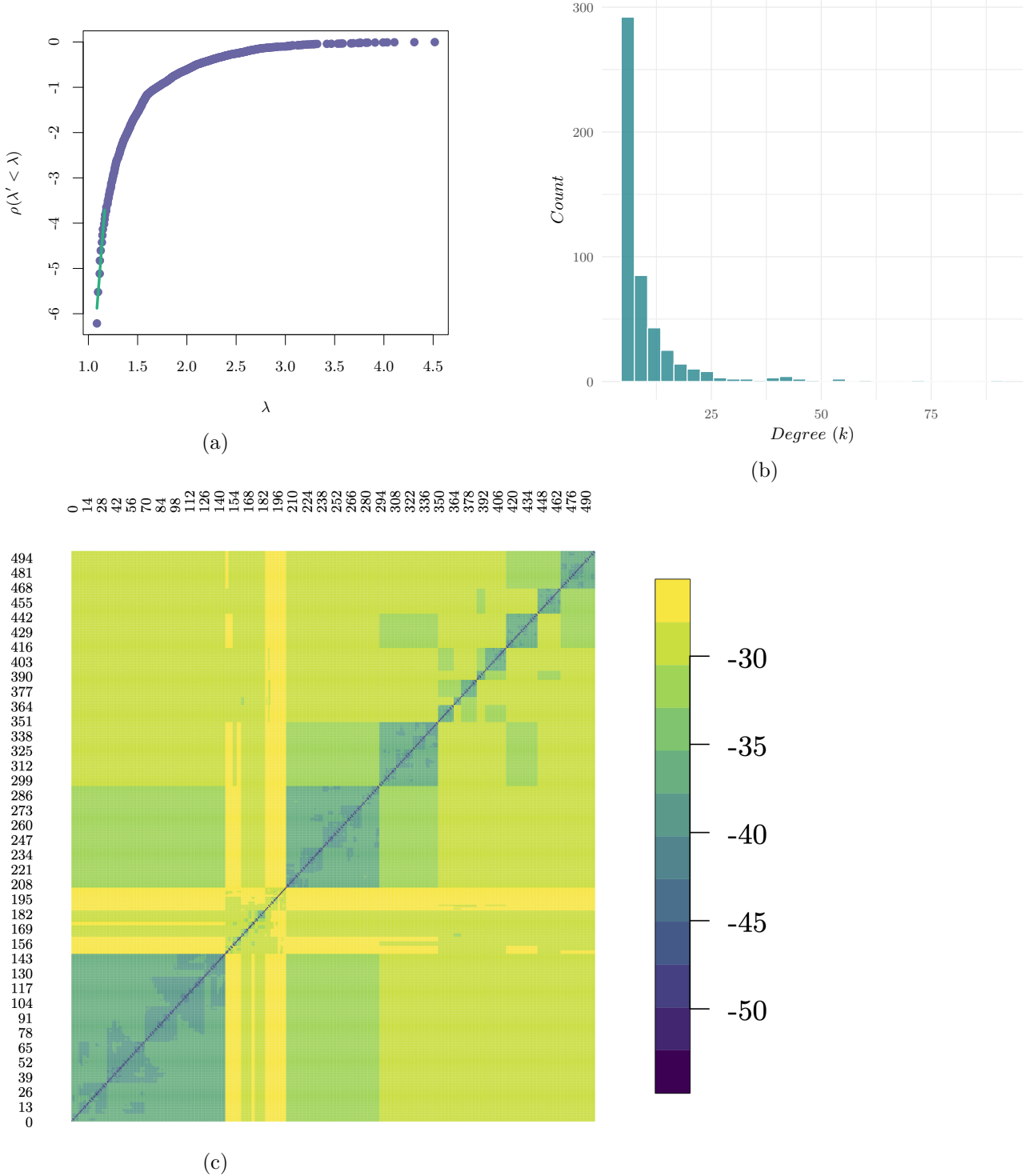


Figure 10: The figures show the recovered spectral density  $d_s = 45.70$ , the non-homogenous degree distribution of graph  $\mathcal{G}_1$ , as well as the heatmap of the pairwise logarithmic difference of  $|u_{1,v}(\mathcal{G}_1) - u_{1,v}(\mathcal{G}_2)|$  for Albert-Barabasi graphs with  $N = 500$ , and a power-law coefficient of 2.72.

## 7.6 Watts-Strogatz graphs

We apply our framework on Watts-Strogatz graphs of size  $N = 500$  with non-homogeneous degree distributions.  $\rho$ , the degree distribution, and  $C$  are shown in Figure 11.

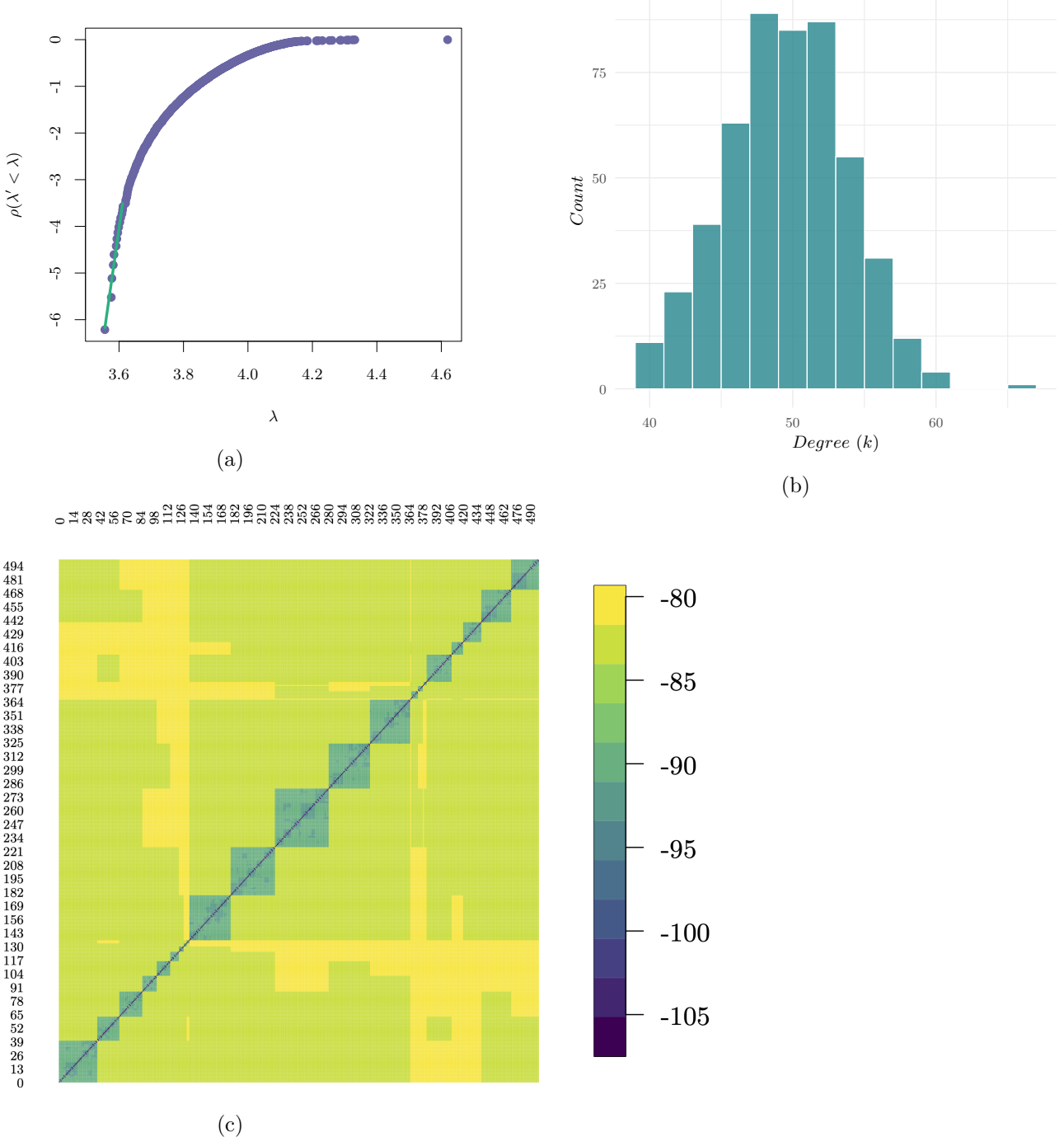


Figure 11: The figures show the recovered spectral density  $d_s = 93.13$ , the non-homogenous degree distribution of graph  $\mathcal{G}_1$ , as well as the heatmap of the pairwise logarithmic difference of  $|u_{1,v}(\mathcal{G}_1) - u_{1,v}(\mathcal{G}_2)|$  for Watts-Strogatz graphs of  $N = 500$ , mean degree  $k_{mean} = 50$ , and rewiring probability of 0.5.

## 7.7 Erdos-Renyi graphs

We apply our framework on Erdos-Renyi graphs of size  $N = 500$  with non-homogeneous degree distributions.  $\rho$ , the degree distribution, and  $C$  are shown in Figure 12.

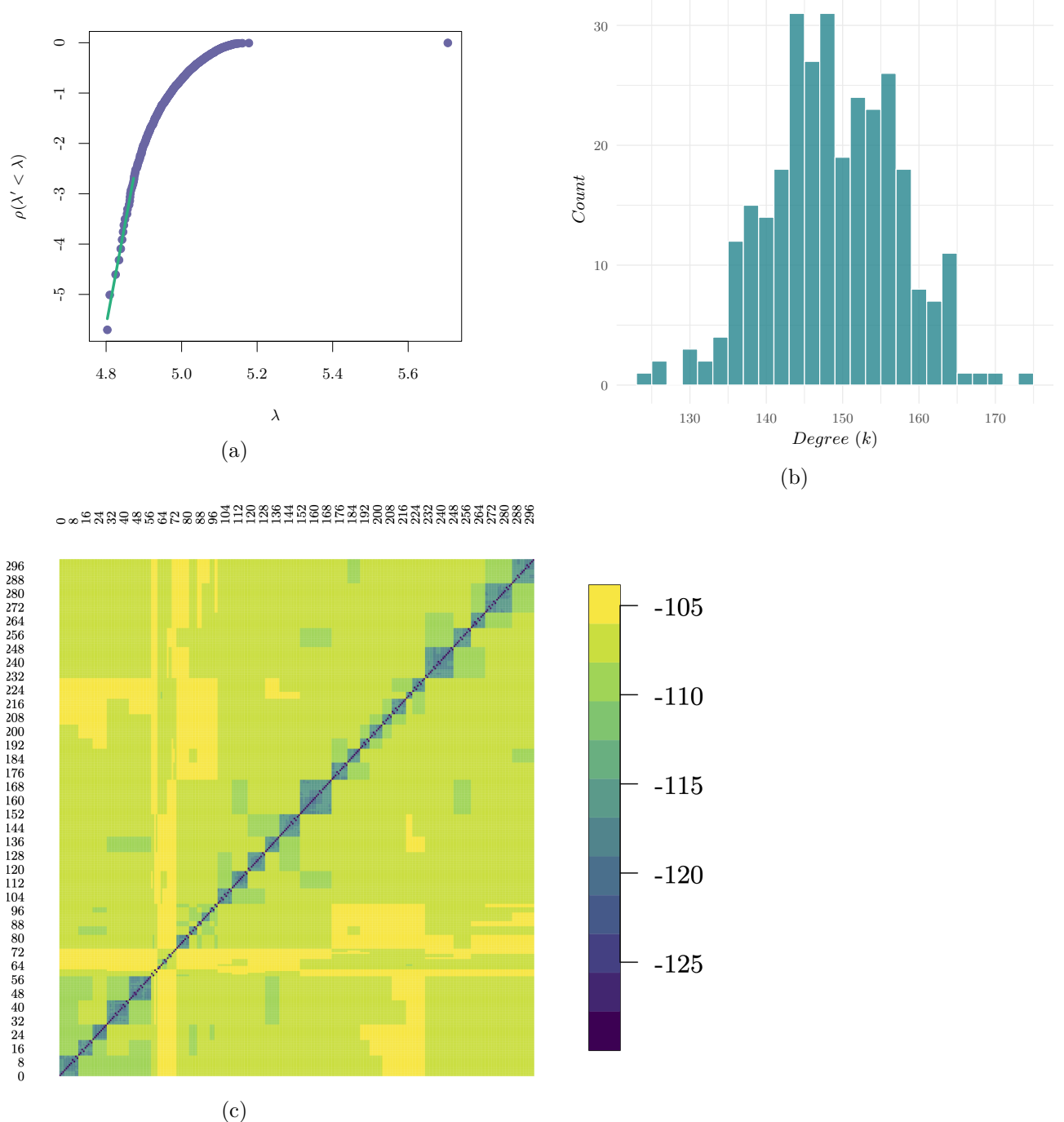


Figure 12: The figures show the recovered spectral density  $d_s = 75.78$ , the non-homogenous degree distribution of graph  $\mathcal{G}_1$ , as well as the heatmap of the pairwise logarithmic difference of  $|u_{1,v}(\mathcal{G}_1) - u_{1,v}(\mathcal{G}_2)|$  for Erdos-Renyi graphs of  $N = 500$  and an edge probability of 0.5.

## 7.8 Tree graphs

We apply our framework on tree graphs of size  $N = 500$ .  $\rho$ , the degree distribution, and  $C$  are shown in Figure 13.

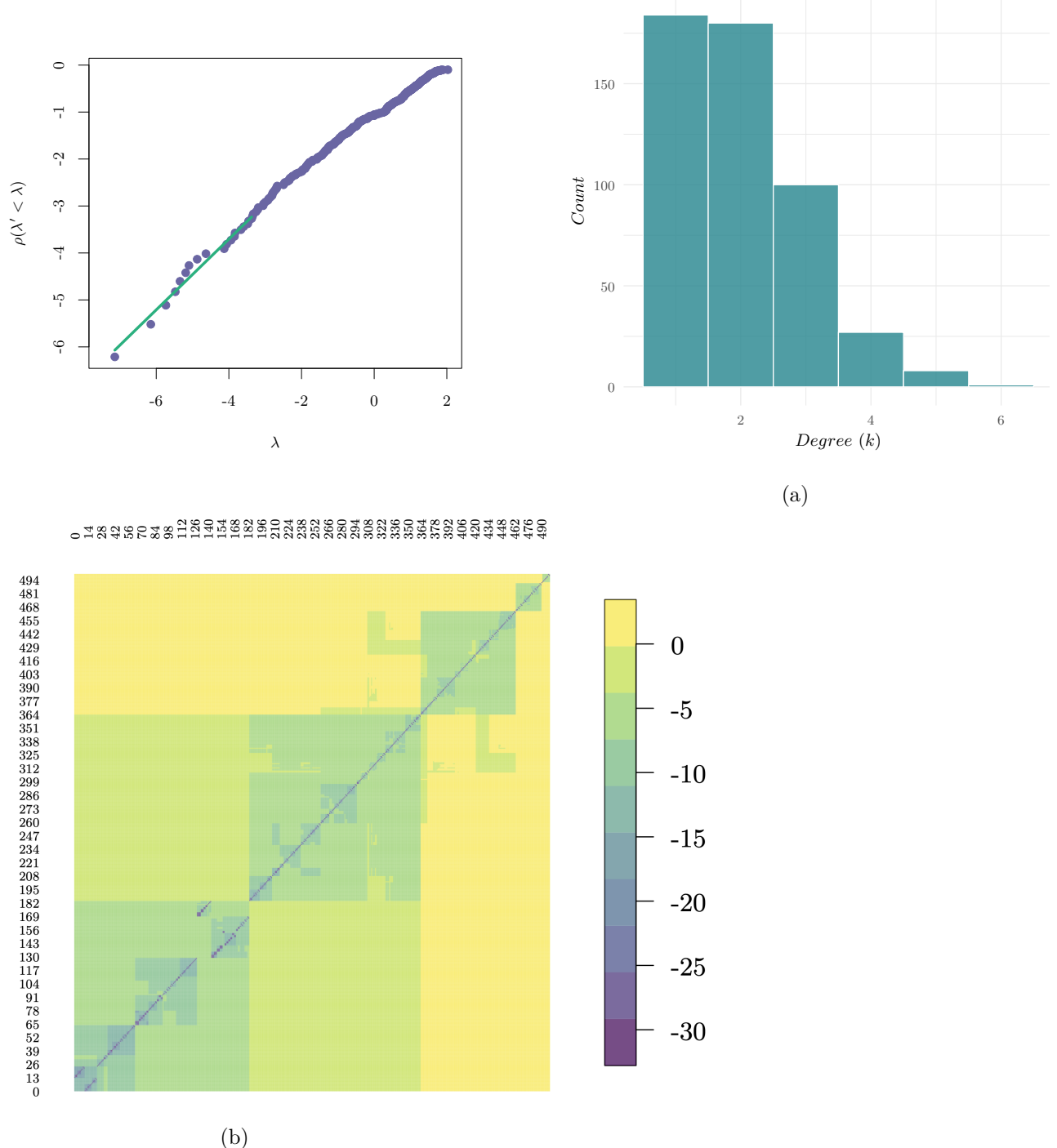


Figure 13: The figures show the recovered spectral density  $d_s = 1.45$ , the non-homogenous degree distribution of graph  $\mathcal{G}_1$ , as well as the heatmap of the pairwise logarithmic difference of  $|u_{1,v}(\mathcal{G}_1) - u_{1,v}(\mathcal{G}_2)|$  for Trees of  $N = 500$ .

## 7.9 Paley graphs

We finally apply our formalism on Paley graphs, for which we show the non-augmented and augmented versions in Figure 14. We start by evaluating curvature on the augmented graphs shown in Figure 15. They exhibit total symmetry in curvature among the original nodes, on the one hand, and the auxiliary on the other.

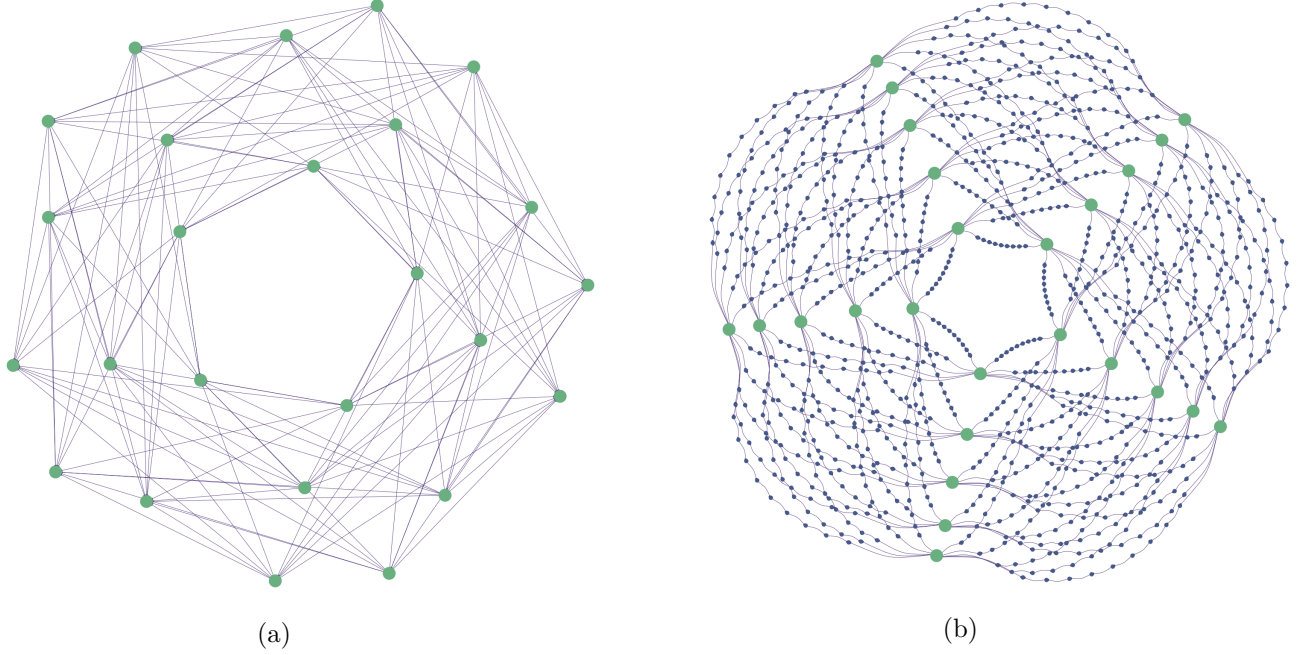


Figure 14: Figure (a) shows the original Paley graph, while (b) shows the augmented that ensures a power-law behavior of the eigenvalue density  $\rho(\lambda' < \lambda)$ .

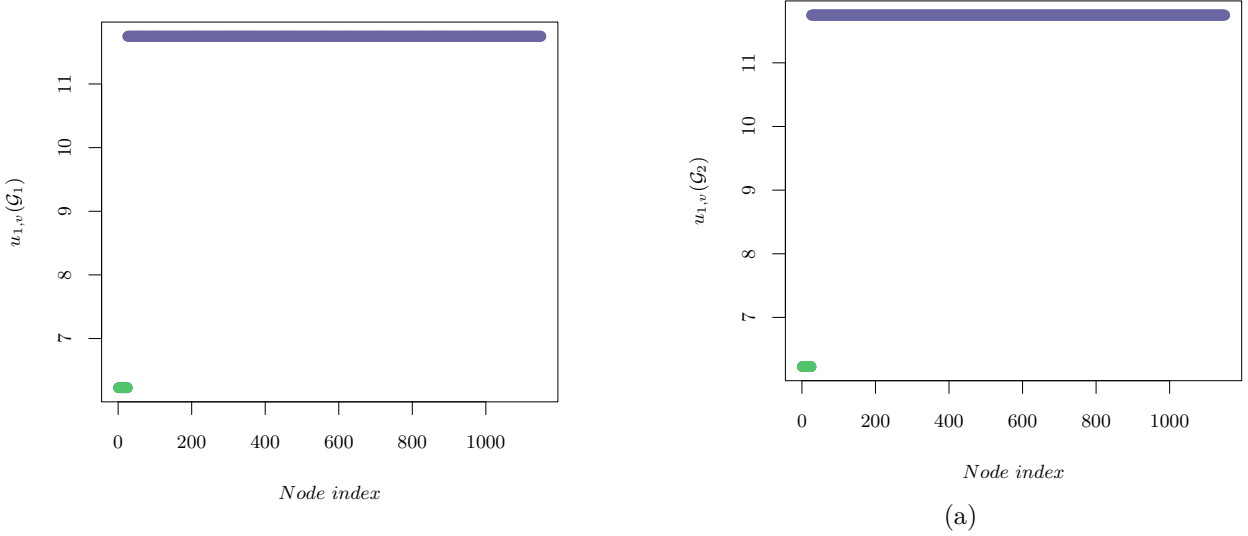


Figure 15: The figure shows the original Paley curvatures  $u_{1,v}(\mathcal{G}_1)$  and  $u_{1,v}(\mathcal{G}_2)$  clearly identifying the green nodes of Figure 14(b).

We show the results of the symmetry breaking construction for vertex identification in Figure 16. We then compute curvatures associated with the resultant graphs shown in Figure 17. They exhibit a clear breaking of symmetry of the green nodes allowing us to identify an isomorphic mapping between the nodes by the values of their sorted curvatures.

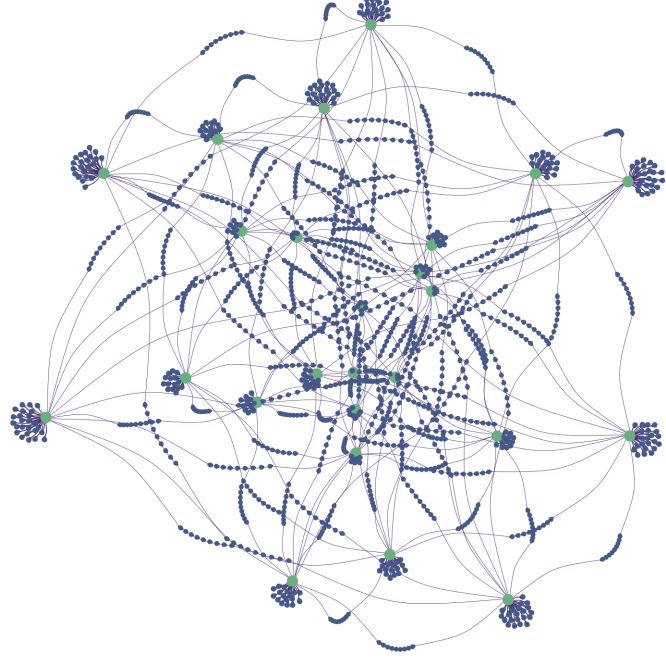


Figure 16: The figure shows the resulting graph of the symmetry breaking construction for vertex identification.

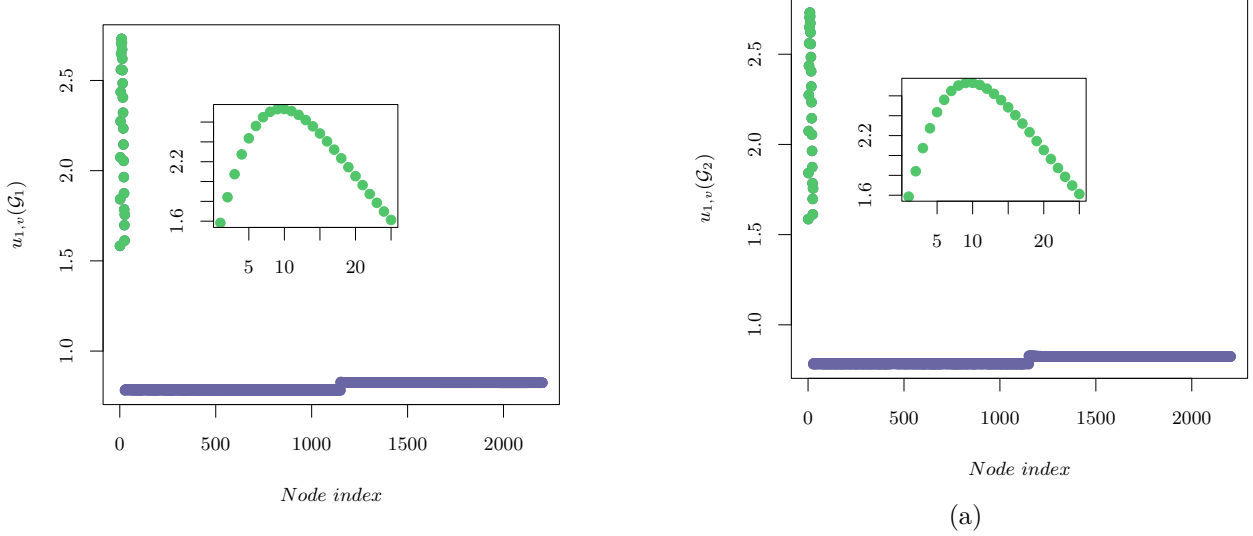


Figure 17: The figure shows the curvatures  $u_{1,v}(\mathcal{G}_1)$  and  $u_{1,v}(\mathcal{G}_2)$  after applying the vertex identification algorithm, which clearly separates the green nodes of Figure 14(b).

## 8 Conclusion and future work

In this work, we introduced a new algorithmic approach to the graph isomorphism problem based on spectral geometry. By extracting curvature information from the graph Laplacian via heat-kernel-based constructions and organizing this information into multi-scale, BFS-based curvature signatures, we developed a principled symmetry-breaking mechanism that goes beyond classical spectral invariants. While this method does not constitute a proof that graph isomorphism admits a polynomial-time algorithm, it demonstrates that geometric information derived from spectral data can be surprisingly effective in practice. In extensive experiments across all graph families generated by standard generators, the algorithm correctly resolved every instance tested.

These results suggest that curvature-based spectral features capture structural distinctions that are invisible to eigenvalues alone. More broadly, they reveal a previously unexplored connection between graph isomorphism and discrete spectral geometry, complementing existing combinatorial, refinement-based, and group-theoretic approaches. Viewed through this lens, vertex identification becomes a local-to-global process: rich local geometric signatures induce a global correspondence between graphs.

Several directions for future work naturally arise. First, while the current experimental evaluation is broad, it is far from exhaustive. A primary goal is to scale the empirical study substantially, both in graph size and in diversity of graph families. Implementing the algorithm on GPUs would allow rapid computation of spectral quantities and heat-kernel features, enabling the exploration of much larger instances and denser parameter regimes. Such large-scale experimentation is essential to stress-test the method, identify potential failure modes, and better characterize the classes of graphs on which curvature-based invariants are most effective.

Second, a deeper theoretical understanding of the method is needed. At present, the success of curvature-based signatures as symmetry-breaking tools is supported empirically but not yet fully explained. An important direction is to analyze how these signatures interact with graph automorphism groups, eigenvalue multiplicities, and refinement hierarchies, and to determine under what conditions they yield provably unique or canonical vertex distinctions. Establishing formal guarantees, such as sufficient conditions for completeness or connections to known tractable graph classes, would significantly strengthen the theoretical foundations of this approach.

Finally, the ideas developed here are not specific to graph isomorphism. Spectral geometry offers a general framework for extracting geometric structure from discrete objects, and curvature-based features may be useful in a wide range of algorithmic problems where symmetry and structural ambiguity play a central role. Potential applications include graph canonization, clustering, network alignment, and related problems where distinguishing subtle structural differences is critical. Exploring these broader applications may reveal that curvature, much like eigenvalues and eigenvectors before it, becomes a fundamental primitive in the algorithmic toolkit.

Taken together, we view this work as an initial step toward a richer interaction between spectral geometry and algorithm design. Whether or not curvature ultimately leads to polynomial-time graph isomorphism, it opens a new direction that is both practically promising and theoretically intriguing.

## References

- [1] Alfred V. Aho, John E. Hopcroft, and Jeffrey D. Ullman. *The Design and Analysis of Computer Algorithms*. Addison-Wesley, 1974.

- [2] Noga Alon and Vitali D. Milman.  $\lambda_1$  isoperimetric inequalities for graphs, and superconcentrators. *Journal of Combinatorial Theory, Series B*, 38(1):73–88, 1985.
- [3] László Babai. On the complexity of canonical labeling of strongly regular graphs. *SIAM Journal on Computing*, 9(1):212–216, 1980.
- [4] László Babai. Graph isomorphism in quasipolynomial time. *Proceedings of the 48th Annual ACM Symposium on Theory of Computing*, pages 684–697, 2016.
- [5] László Babai, Dmitry Yu. Grigoryev, and David M. Mount. Isomorphism of graphs with bounded eigenvalue multiplicity. *Proceedings of the Fourteenth Annual ACM Symposium on Theory of Computing*, pages 310–324, 1982.
- [6] J. S. Caughman and J. J. P. Veerman. Kernels of directed graph laplacians. *Electronic Journal of Combinatorics*, 13(R39):1–13, 2006.
- [7] Fan R. K. Chung. *Spectral Graph Theory*, volume 92 of *CBMS Regional Conference Series in Mathematics*. American Mathematical Society, Providence, RI, 1997.
- [8] Karamatou Yacoubou Djima and Ka Man Yim. Power spectrum signatures of graphs. *arXiv preprint*, page arXiv:2503.09660v1, 2025.
- [9] Miroslav Fiedler. Algebraic connectivity of graphs. *Czechoslovak Mathematical Journal*, 23(2):298–305, 1973.
- [10] Robin Forman. Bochner’s method for cell complexes and combinatorial ricci curvature. *Discrete and Computational Geometry*, 29(3):323–374, 2003.
- [11] Martin Grohe. Graph isomorphism, logic, and polynomial time. *Bulletin of Symbolic Logic*, 21(1):1–45, 2015.
- [12] John E. Hopcroft and James K. Wong. A linear time algorithm for isomorphism of planar graphs. *Proceedings of the Sixth Annual ACM Symposium on Theory of Computing*, pages 172–184, 1974.
- [13] Eugene M. Luks. Isomorphism of graphs of bounded valence can be tested in polynomial time. *Journal of Computer and System Sciences*, 25(1):42–65, 1982.
- [14] Russell Merris. Laplacian matrices of graphs: a survey. *Linear Algebra and its Applications*, 197–198:143–176, 1994.
- [15] Sara Najem, Dima Mrad, and Mohammad Elsayed. Geometric features of higher-order networks via the spectral triplet. *arXiv preprint arXiv:2509.04311*, 2025.
- [16] Yann Ollivier. Ricci curvature of markov chains on metric spaces. *Journal of Functional Analysis*, 256(3):810–864, 2009.
- [17] Dan Raviv, Ron Kimmel, and Alfred M. Bruckstein. Graph isomorphisms and automorphisms via spectral signatures. *IEEE Transactions on Pattern Analysis and Machine Intelligence*, 35(8):1985–1993, 2013.
- [18] Jian Sun, Maks Ovsjanikov, and Leonidas Guibas. A concise and provably informative multi-scale signature based on heat diffusion. *Computer Graphics Forum*, 28(5):1383–1392, 2009.

- [19] Joaquín J Torres and Ginestra Bianconi. Simplicial complexes: higher-order spectral dimension and dynamics. *Journal of Physics: Complexity*, 1(1):015002, 2020.
- [20] Ryuhei Uehara, Seinosuke Toda, and Akira Nagoya. Tractable and intractable instances of the graph isomorphism problem. *Theoretical Computer Science*, 349(2):243–256, 2005.